REVIEW ARTICLE
https://doi.org/10.1038/s41558-019-0456-2

nature climate change

Contributions of GRACE to understanding climate change

Byron D. Tapley[1], Michael M. Watkins[2], Frank Flechtner[3,9], Christoph Reigber[3], Srinivas Bettadpur[1], Matthew Rodell[4], Ingo Sasgen[5*], James S. Famiglietti[6], Felix W. Landerer[2], Don P. Chambers[7], John T. Reager[2], Alex S. Gardner[2], Himanshu Save[1], Erik R. Ivins[2], Sean C. Swenson[8], Carmen Boening[2], Christoph Dahle[3], David N. Wiese[2], Henryk Dobslaw[3], Mark E. Tamisiea[1] and Isabella Velicogna[2]

Time-resolved satellite gravimetry has revolutionized understanding of mass transport in the Earth system. Since 2002, the Gravity Recovery and Climate Experiment (GRACE) has enabled monitoring of the terrestrial water cycle, ice sheet and glacier mass balance, sea level change and ocean bottom pressure variations, as well as understanding responses to changes in the global climate system. Initially a pioneering experiment of geodesy, the time-variable observations have matured into reliable mass transport products, allowing assessment and forecast of a number of important climate trends, and improvements in service applications such as the United States Drought Monitor. With the successful launch of the GRACE Follow-On mission, a multi-decadal record of mass variability in the Earth system is within reach.

Global observations of water and ice mass redistribution in the Earth system at monthly to decadal time scales are critical for understanding the climate system and investigating its changes. Together with other observations, they provide information on the Earth's energy storage, ocean heat content, land surface water-storage, and ice-sheet response to global warming. Interactions between the different climate system components involve mass variations in continental surface and sub-surface water storage (rivers, lakes, ground water, snow cover, polar ice sheets and mountain glaciers), as well as the mass redistribution within and between ocean and atmosphere. These mass movements are inherent to the evolution of droughts, floods, large-scale ocean currents, ice-sheet and glacier changes, and sea-level rise. Launched in 2002, the Gravity Recovery and Climate Experiment (GRACE) satellite mission[1] added a unique component to the existing suite of Earth observations: time-resolved gravity measurements of global-mass redistribution, a fundamental building block crucial to understanding the complex interactions and transitions involved in today's changing climate.

Measurement principle of the GRACE mission

The GRACE mission was launched on 17 March 2002, in a collaboration between the National Aeronautics and Space Administration (NASA) and the German Aerospace Centre (DLR), in response to recommendations resulting from decades of study[2,3]. The primary objective of GRACE was to apply monthly aggregated measurements of the Earth's gravity field to track mass changes in the hydrosphere, cryosphere and oceans[4]. In contrast to single satellite approaches with one dedicated sensor, GRACE uses a constellation of two satellites, orbiting one behind the other, featuring a suite of measurement systems (see Box 1). The fundamental measurement is derived from micron level tracking of the satellite-to-satellite distance, which varies due to individual gravitational attractions on the satellites as they pass over the Earth's surface[1].

After a month, the collected measurements allow an estimate of a global spherical harmonic model of the Earth's gravity field, which is then used to estimate mass changes on the Earth's surface. Processing choices made by the Science Data System (SDS) centres and its users can lead to differences between mass time series determined from the GRACE measurements[5–7]. To enhance the use of GRACE data in diverse Earth science applications, SDS centres now provide quality-controlled, gridded and basin-integrated mass change products (Level 3 data, see 'Data availability').

Success of a pioneering mission. The GRACE mission ended on 12 October 2017, due to battery failure, after providing paradigm-shifting near-continuous measurements for over 15 years—ten years longer than the nominal mission lifetime. The mission's data record provides 163 monthly solutions of the time varying gravity field, out of 187 possible months, along with a highly accurate mean field. For the first time, GRACE enabled the quantification of mass trends and mass fluctuations of terrestrial water storage, continental aquifers, and glaciers and ice sheets (Fig. 1), and enlightened our view of large-scale mass redistribution associated with glacial-isostatic adjustment and earthquakes. With this data, GRACE contributed to quantifying global and regional changes, from both natural variability and anthropogenic influence, in the hydrological cycle, ice-sheet mass balance, ocean circulation and sea-level change.

[1]Center for Space Research, University of Texas, Austin, TX, USA. [2]Jet Propulsion Laboratory, California Institute of Technology, Pasadena, CA, USA. [3]Department of Geodesy, GFZ German Research Centre for Geosciences, Telegrafenberg, Potsdam, Germany. [4]Hydrological Sciences Laboratory, NASA Goddard Space Flight Center, Greenbelt, MD, USA. [5]Division of Climate Sciences, Alfred Wegener Institute, Bremerhaven, Germany. [6]Global Institute for Water Security, University of Saskatchewan, Saskatoon, Saskatchewan, Canada. [7]College of Marine Science, University of South Florida, St. Petersburg, FL, USA. [8]Climate and Global Dynamics Laboratory, National Center for Atmospheric Research, Boulder, CO, USA. [9]Department of Geodesy and Geoinformation Science, Technical University Berlin, Berlin, Germany. *e-mail: ingo.sasgen@awi.de

Box 1 | GRACE and GRACE-FO measurement is implemented by two identical satellites (GRACE A/B) orbiting one behind the other in a near-polar orbit plane

The along-track separation is kept within a range of 220 ± 50 km. The satellites experience positive and negative, gravitationally induced, along-track accelerations due to the varying mass distribution below them. Each satellite will experience the effects of the local mass at slightly different times causing a differential acceleration. The differential acceleration, in turn, causes distance (range) variations and velocity differences Δv that are proportional to the mass attraction related to the gravitational potential, U. The relative distance between the satellites is measured with micron-level precision by a high accuracy dual frequency K-band inter-satellite ranging system. An accurate three-axis accelerometer measures the effects of all non-gravitational forces acting on each satellite, including atmospheric drag, direct and Earth-reflected solar radiation pressure, and thrusting. A GPS receiver on each satellite provides position and time synchronization, and a dual star camera assembly gives information on the satellites' orientation in space. The satellites overfly the entire Earth surface within approximately 30 days, allowing monthly estimates of a global gravity model with a surface spatial resolution of, typically, 300 km with an accuracy of 2 cm (ref. [128]). Image adapted from ref. [129], NASA.

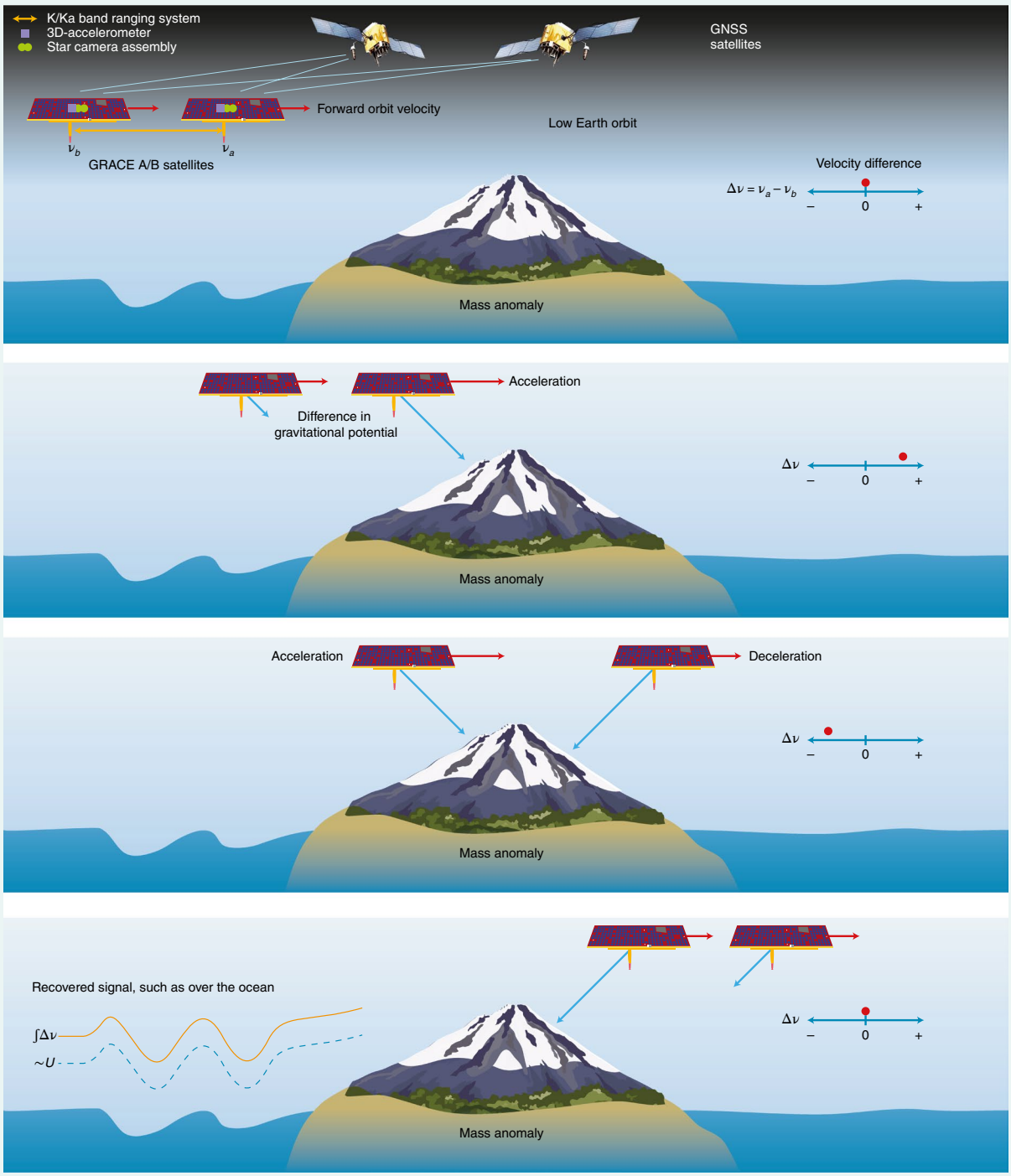

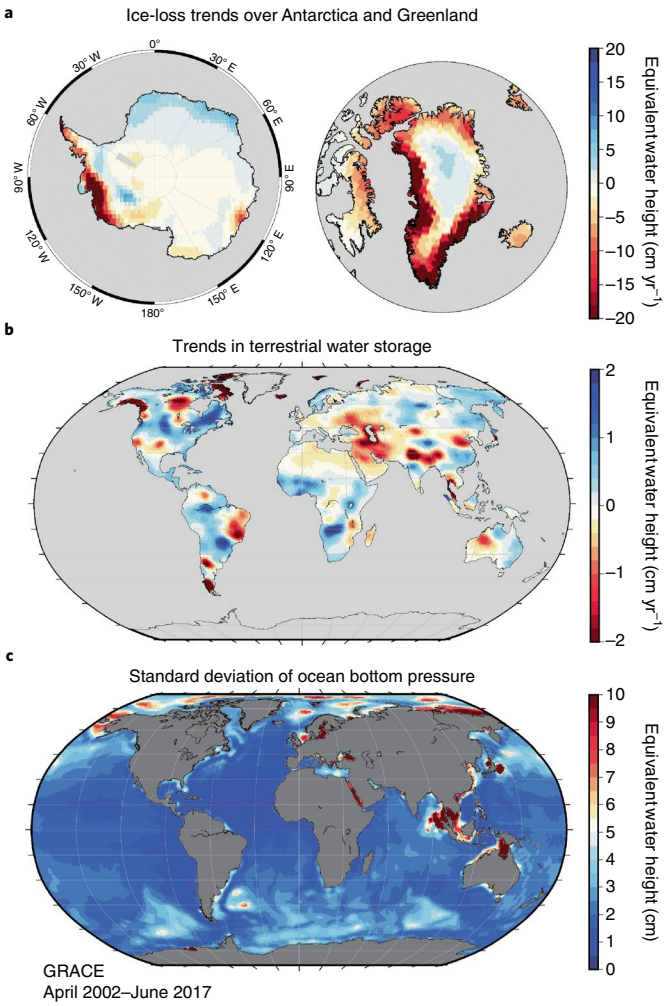

Fig. 1 | Global representation of trends and variability in ice and water mass recovered by GRACE over 15 years. a, The trend maps over Antarctica, Greenland and part of the Arctic mainly represent changes in ice mass. **b**, The trend map mainly represents changes in the terrestrial water storage, as well as large trends related to glacier ice-loss from continental areas, such as Alaska, Patagonia and the Canadian Arctic. The trends of the terrestrial water storage are partially related to climate variability causing floods and droughts, but also reflect, for example, long-term changes in groundwater depletion by human activity. **c**, Standard deviation of the ocean bottom pressure obtained from the high-resolution information of the ocean background model used in the GRACE data processing, plus corrections of the background model from GRACE (ref. [109]), which are particularly relevant in the southern oceans and the Arctic Ocean[5]. For **a**,**b**, red represents mass loss and blue represents mass gain. In **c**, the colour scales represent variability, with the highest variability shown in red. The data source is CSR RL05M Mascons[5]. A GIA correction[125] has been subtracted in **a** and **b**. Details on the data shown are presented in 'Data availability'.

This Review highlights some representative breakthroughs, selected from numerous scientific publications, based on GRACE observations in the fields of cryosphere, hydrology and ocean sciences, as well as in service applications.

Ice sheets and glaciers

Today's changes in continental ice-mass sensitively indicate active transitions in the atmosphere and oceans that have, in the past centuries to millennia, sustained ice sheets and glaciers as stable geographic features. As the oceans and atmosphere have warmed over the past decades, ice sheets and glaciers have experienced increased melting[8,9]. Outlet glaciers that terminate in the ocean have experienced increased subaqueous melting and reduced buttressing at glacier fronts that have increased rates of ice-dynamic discharge. These changing oceanic and atmospheric conditions have led to sharp increases in rates of mass-loss from nearly all glaciered regions on Earth[10], causing more than half of the global mean sea-level rise[11].

Without GRACE, satellite observations are restricted to measuring changes in the surface height of the ice sheet with radar (ERS-1/2, Envisat or CryoSat-2) and laser (ICESat 1/2) altimetry, which are influenced by changes in the properties of the surface layer and firn compaction, and only provide indirect measurements of the net mass change (comprising precipitation, evaporation, runoff and ice discharge). Alternatively, the components of the net mass change can be addressed by estimating precipitation and runoff with regional climate models and measuring discharge with interferometric synthetic aperture radar (InSAR)[12] and optical feature/speckle tracking. GRACE provided the first direct measurement of ice mass change. While altimetry estimates are commonly restricted to multi-annual trends of height-change due to sampling issues and their sensitivity to snow at the ice-sheet surface, GRACE-derived ice-sheet and glacier mass changes are obtained with an unprecedented temporal resolution of one month. The long-term mass trends that are derived from GRACE for ice sheets are less influenced by sampling issues, or unknown surface properties, than other methods[10]. However, particularly for Antarctica, problems remain in correcting for often poorly known mass-redistribution induced by the glacial-isostatic adjustment (GIA)—a slow rebound of the Earth's underlying lithosphere and mantle following readjustment from past ice-sheet retreat[13,14].

Mass balance of Greenland and Antarctica. Within two years after mission launch, GRACE data analysis revealed a clear signal of ice-mass loss in Greenland and Antarctica[15,16]. Mass trends became more robust and accurate with extension of the mission measurement period to longer than five years; the increased quality of the gravity field solutions themselves also contributed to this robustness[17]. Further, GRACE analysis isolated the largest mass imbalance in southeast Greenland[6] and the Amundsen Sea Embayment, West Antarctica[18]. Over the GRACE life span, the mass loss in Greenland encompassed the ice-sheet's entire margin. In Antarctica, the Amundsen Sea Embayment of the ice-sheet dominates the mass lost in response to changed oceanic conditions (Fig. 1).

The Greenland GRACE time series are in general accord with independent estimates derived from satellite altimetry and the component approach. This allowed the inference that 60% of the total mass-loss is due to enhanced melt production in response to Arctic warming trends, while 40% is due to an increase in ice-dynamic outflow[8,12,19]. With the increasing length of the GRACE time series, acceleration of mass loss was inferred to be statistically significant for some regions of both ice sheets[20]. However, although an acceleration of mass-loss is expected as the ice sheets adapt to increasing global temperatures, Wouters et al.[21] showed that natural variability of the ice-sheet mass can lead to misinterpretation of the accelerations deduced from satellite records covering one or two decades. Recent years have shown reduced annual mass-loss of the Greenland ice sheet (Fig. 2), decreasing the values of acceleration detected through the year 2012 (ref. [22]). For many regions, the significance and cause of the variations in the mass change are still a matter of debate.

As an update to previous studies, we note that during the period of April 2002 to June 2017, Greenland showed a negative average annual balance of −258 ± 26 Gt yr^{-1} (uncertainties represent two standard deviations, 2σ; propagated and GIA uncertainty), with a measured year-to-year variability of ±137 Gt yr^{-1} (±53% with

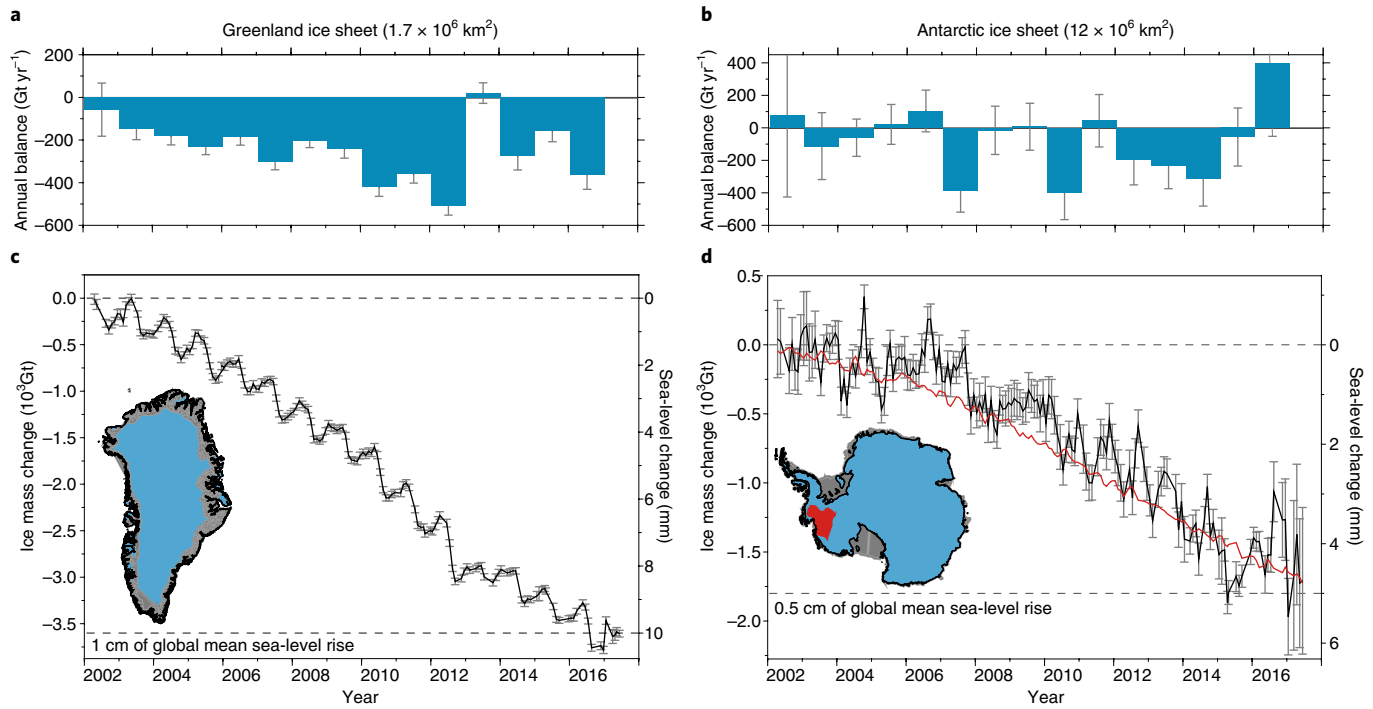

Fig. 2 | GRACE observations of mass change of the Polar ice sheets between April 2002 and June 2017. a,**b**, Annual mass balance of the Greenland Ice Sheet (**a**) and the Antarctic Ice Sheet (**b**). **c**,**d**, Time series of mass change of the Greenland Ice Sheet (**c**) and the Antarctic Ice Sheet (**d**), as well as the region of the Amundsen Sea Embayment only (red). Dashed lines indicate the equivalent global mean sea-level rise by 1 cm (**c**) and 0.5 cm (**d**). Updated from Sasgen et al.[19,126]. The data source is CSR RL05. Details on the data shown are presented in 'Data availability'.

respect to the average). For the Antarctic ice sheet, the average annual mass balance determined by GRACE is −137 ± 41 Gt yr^{-1} (2σ; propagated and GIA uncertainty), with a considerably larger year-to-year variability of ±208 Gt yr^{-1} (Fig. 2). The largest ice-mass loss is caused by a speed-up of glaciers and ice streams feeding into the Amundsen Sea Embayment, for which GRACE recorded mass changes of −120 ± 14 Gt yr^{-1} (2σ) with an acceleration of −7 ± 2 Gt yr^{-1} (2σ; Fig. 2).

Mass signatures of changes in global atmospheric circulation. Apart from the long-term trends, GRACE enabled a direct relation of inter-annual fluctuations in the mass of ice sheets and the global variability in atmospheric circulation patterns. For example, the anomalous melt event in Greenland, in 2012, (Fig. 2) was driven by the advection of warm air from the mid-latitudes due to strong atmospheric blocking conditions over Greenland[23]. GRACE showed that estimates of melt-enhanced mass-loss were doubled in 2012 (−543 ± 27 Gt yr^{-1}, 2σ), compared to the average for 2003–2011 (Fig. 2).

It has also been shown that West Antarctic accumulation fluctuations from GRACE correlate well with El Niño Southern Oscillation (ENSO)-modulated moisture-flux to the continent[24]. Atmospheric pressure patterns create southward transport of moisture that delivered snowfalls of 300 Gt in 2009 and 2011 along the Atlantic Sector of the Antarctic ice sheet[25]. With the extended mission data, Mémin et al.[26] used GRACE measurements to identify a periodic signal of about four to six years in the coastal precipitation, connected to the Antarctic Circumpolar Wave and ENSO. For the cold regions of the Earth, GRACE measurements of large-scale accumulation variations are important for validating the net continental balance of moisture-flux in weather and climate models[27], which are otherwise largely dependent on sparse and expensive in-situ networks.

Monitoring glacier fluctuations and trends with global coverage. GRACE has proven to be an invaluable tool for the challenging measurement of mass trends of glacier regions outside Greenland and Antarctica. Even though glaciers are highly localized features, the imprint of their collective imbalance is easily detected in the regional gravity field. Advantageous for recovering these small-scale features is the higher spatial resolution of GRACE in high latitudes, which is possible with denser ground-track spacing. Thus, GRACE helped identify a large bias in the in situ glacier-monitoring network, which traditionally aggregates individual measurements to estimate glacier contributions to sea-level rise[9]. Furthermore it has been shown that GRACE-derived trends in glacier mass are in accord with satellite laser altimetry[28,29] and surface-mass-balance models[29,30]. Regionally, trends were successfully quantified for Alaska[31,32], Patagonia[33,34], Iceland, the Canadian Arctic and Svalbard[17], and later for all glaciered regions[9,35].

Terrestrial water storage

Among the most impactful contributions of the GRACE mission has been in the unveiling of Earth's changing freshwater landscape, which has profound implications for water, food and human security. Global estimates of GRACE trends suggest increasing water storage in high and low latitudes (wetting), with decreased storage in mid-latitudes (drying)[36,37] (Fig. 1). Though the GRACE record is relatively short, this observation of large-scale changes in the global hydrological cycle has been an important early confirmation of the changes predicted by climate models through the twenty-first century[38,39]. Nevertheless, projections of future water availability remain quite model-dependent and require a systematic evaluation of soil moisture trends from models, such as the Coupled Model Intercomparison Project Phase 5 (CMIP5), with GRACE and other measurements. Wetting in high and low latitudes, drying mid-latitudes and falling water tables in mid-latitude aquifers[40], all indicate

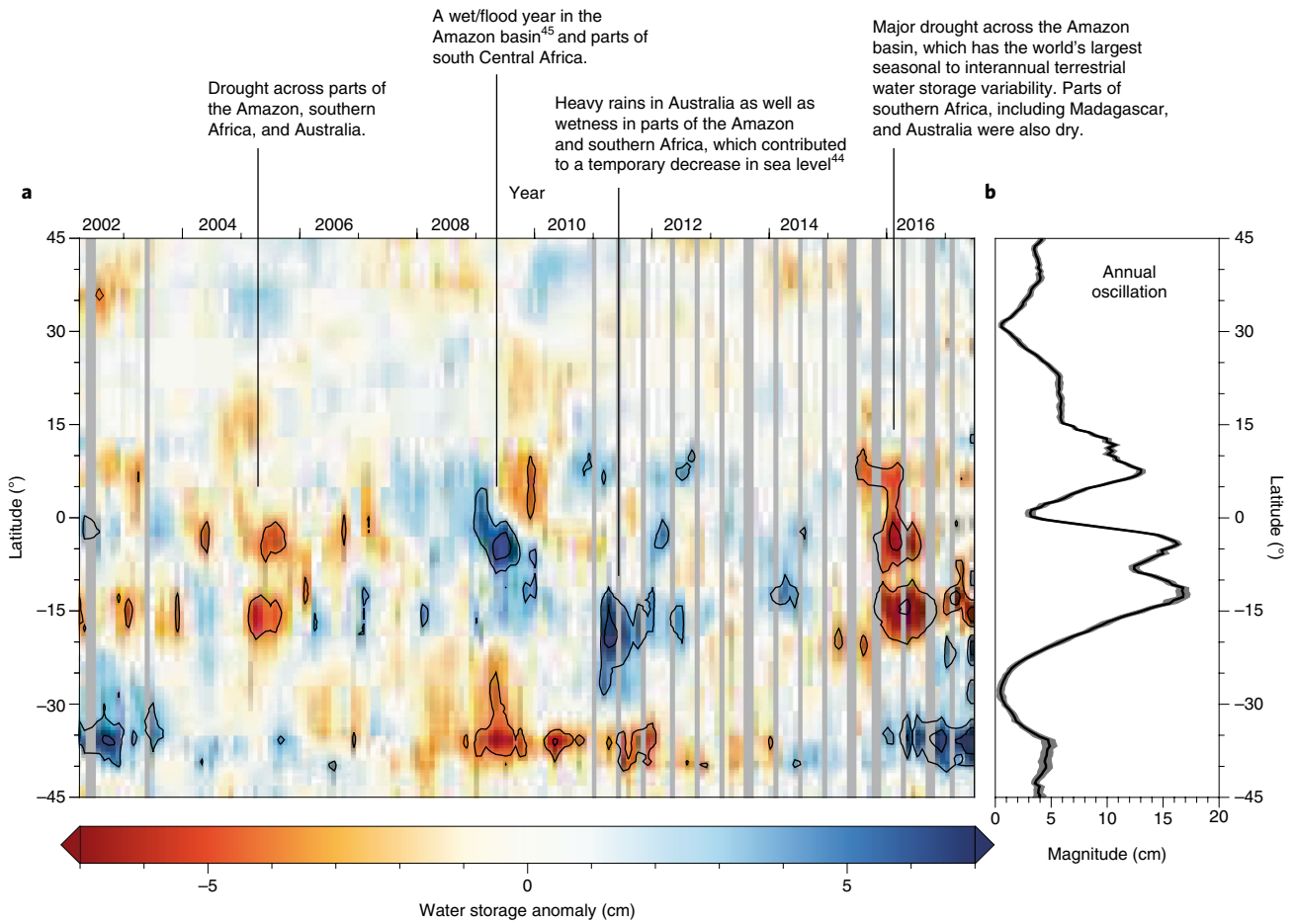

Fig. 3 | GRACE zonal mean of terrestrial water storage anomalies for April 2002 to June 2017. a, The time series of anomalies after subtracting an annual periodic component, offset and linear trend. Contour levels are at ± 4 and ± 8 cm equivalent water height. **b**, The magnitude of the annual oscillation. Based on CSR RL05M Mascons[5]. Details on the data shown are presented in 'Data availability'.

potential changes in future access to fresh water, with implications for the sustainability of water for human consumption, irrigation and food security, and industrial uses. Of the world's 37 largest aquifer systems, 13 were found to be suffering critical depletion during the GRACE observational period[40].

Terrestrial water storage and climate variability. Measurements of continental water mass change from GRACE have been examined in the context of climate variability in several recent studies[36,37,41–44]. As an example, Fig. 3 (right panel) shows that the GRACE-derived zonal mean of the annual amplitude of terrestrial water storage (TWS)—that is the sum of snow, ice, surface water, soil moisture and groundwater—has a range of ±17 cm equivalent water height. As indicated in Fig. 3, climate driven perturbations of annual TWS variation are often associated with flood[45,46] and drought[47–49] years in low to mid-latitudes. GRACE TWS data also helped to establish the current state of the water cycle[50] so that ongoing and future hydroclimatic change can be detected. Further, since 2011 such zonal mean water mass plots have been included in annual climate reports as indicators of TWS and groundwater variability[51].

The importance of terrestrial water storage variability in understanding climate is also exemplified by the fact that the global sea level record contains substantial annual variability around an underlying secular trend. Natural variability in TWS can be a significant source or sink in the global ocean mass budget, of similar order to the Greenland Ice Sheet, which contributed on average in the GRACE period 0.7 mm each year to sea-level rise (Fig. 2). The fluctuations in TWS influences on sea-level range from interannual to decadal time scales[52], masking or augmenting the underlying trend[22,36], or even reversing the sign of, the rate of sea-level rise when more water is stored on the continents[46]. This interplay between land-water storage and sea level is of critical importance in interpreting the global sea-level record.

A recent study correlated annual variations in TWS with the rate of carbon uptake by land[53]. The study concluded that the growth rate of atmospheric CO_2 is faster during dry years than during wet years, and that terrestrial water storage is a better indicator of these rates than precipitation. This fascinating development further demonstrates the interdisciplinary utility of the GRACE measurements and suggests pathways for the improvement of climate models.

Detecting trends of anthropogenic groundwater depletion. Embedded within the drying mid-latitudes, hot spots for water-loss during the GRACE mission emerge (Fig. 1), many of which correspond to the world's major aquifer systems. GRACE-derived changes have enabled large-scale water balance closure[50,54,55] and the first-ever estimates of groundwater storage changes from space[56,57]. These studies confirm excessive rates of groundwater depletion from individual aquifers[58–63] around the world[37,40,64,65]. Rodell et al.[37] provide a comprehensive attribution of all the major GRACE-observed hydrological trends to natural variations, anthropogenic climate change or human water-management practices.

Hydrological flux estimation and climate model improvement. TWS change, precipitation, runoff and evapotranspiration are all essential elements of the water cycle and are difficult to quantify, particularly at a global scale. Applying mass conservation, GRACE measurement of the TWS-change allows the derivation of basin-scale flux estimates of evapotranspiration[54,66], river discharge[67], and precipitation minus evapotranspiration[68]. In cold mountainous regions, monthly mean precipitation estimates based on GRACE appear to be advantageous, particularly in the winter months when uncertainties in conventional hydro-meteorological observing systems are large due to the presence of light rain, snow and mixed-phase precipitation[27]. Changes in TWS determined by GRACE and meteorological data are critical for characterizing streamflow in ungauged river basins[69], or for estimating important land–atmosphere interactions.

GRACE trend and amplitude data can be used to validate[70] or calibrate[71] the land component of global climate models (that is, land-surface models) and evaluate their performance. For example, GRACE measurements helped to identify model shortcomings[44,72], and to refine both model structural elements and parameters[70,73,74]. GRACE terrestrial water-storage information now provides a new assimilation component for land-surface model simulation[6,75–80].

The 15-year GRACE record yields insight into the normal range of wet-to-dry-season variation, as well as into excursions from normal wet[45,81] and dry conditions[49,82]. The length of the available time-series reveals a detailed spatial picture of the response of TWS variations to atmospheric energy and water fluxes at sub-seasonal to inter-annual time-scales[42], and to natural climatic oscillations such as El Niño and La Niña[83,84]. Even the estimation of probabilistic return frequencies of regional hydrometeorological extremes is possible[85].

Including GRACE TWS information in a simple model of flood potential can increase early warning lead times by an entire season or more[81]. GRACE-derived drought indices result in longer estimates of drought persistence, relative to indices based only on meteorological fields and surface variables, such as temperature, precipitation and stream flow[49,82]. GRACE-based determination of TWS has contributed to the evaluation of different development stages of a global coupled Earth-System Model designed to facilitate operational climate predictions at time-scales of several months to up to ten years[86].

Sea-level change and ocean dynamics

Sea-level rise is a profound and direct consequence of a warming climate: within this century global mean sea-level rise may accelerate to 10 mm yr^{-1} (ref. [87]), a rate unprecedented during the last 5,000 years[88]. Different physical processes cause this increase: ocean warming leads to volumetric expansion, and continental water and ice-loss causes mass inflow to the ocean. Since 1993, satellite altimetry—primarily the TOPEX/Poseidon and Jason missions—has provided global measurements of sea-surface height, indicating a global average rate of sea-level rise of 3.1 mm yr^{-1} during the past 25 years[22,89] (1993 to 2017). With GRACE and autonomous Argo floats[90], it is possible to directly measure the individual steric and mass change components, respectively, and to assess the sea-level budget with independent measurements on the global scale. By placing a constraint on ocean mass change, GRACE can indirectly constrain the estimate of Earth's energy imbalance, which is a fundamental global metric of climate change[91].

Global mean sea-level budget. Prior to GRACE, the mass component of the sea-level budget was estimated from the difference between altimeter (total) sea-level and thermal-expansion measurements[92]. Despite higher noise-levels in the early data, Chambers et al.[93] estimated ocean mass changes from GRACE. Today, GRACE is used routinely, together with ocean hydrographic profiles from Argo, for examining the global sea-level budget[22], enhancing our understanding of how contributions are changing over time. Figure 4 shows that, from 2005 to 2017, the total sea-level trend of 3.8 ± 0.7 mm yr^{-1} (measured by altimetry) results from a 2.5 ± 0.4 mm yr^{-1} mass inflow (GRACE) and 1.1 ± 0.2 mm yr^{-1} volumetric expansion (Argo) (update from Chambers et al.[94]; see 'Data availability'). However, some discrepancies between the different GRACE products exist, which are discussed in more detail in a recent assessment of the World Climate Research Programme[22].

Resolving long-term accelerations in the data is highly relevant for validating sea-level projections, but requires sufficient knowledge for correction of inter-annual fluctuations arising from natural climate modes. For example, multi-year variations are visible in the altimeter record that are statistically related to ENSO (Fig. 4), but could not be clearly attributed to either heating or ocean mass changes[95]. GRACE provided accurate estimates of the variability caused by the relocation of ocean mass, as well as indentifying its continental source region[46]. Fasullo et al.[96] took this investigation further and used ancillary data to explain how the mass exchange is related to ENSO and other atmospheric drivers, linking the exchanges to the characteristic time scales of terrestrial watersheds.

Ocean heat content and deep-ocean warming. Heat uptake by the ocean is the largest sink for the Earth's energy-increase from rising CO_2 concentrations[91]. Temperature profiles by Argo floats provide a reliable estimate of the ocean-heat content[97]; however, the Argo data coverage excludes ocean depths below 2,000 m and the marginal seas, and is sparse under sea-ice and ice shelves. Together with other observations, GRACE is able to provide an estimate of the ocean heat-budget in an indirect approach. GRACE, altimetry and Argo indicate that most of the warming occurs in the upper 2,000 m of the ocean on a global scale, leading to a thermosteric sea-level rise of 0.9 ± 0.15 mm yr^{-1} between 2005 and 2013 (ref. [98]). The trends at ocean depths below 2,000 m are inferred by subtracting the sum of the total GRACE mass trends and Argo warming trends above 2,000 m, from the altimeter measurements of total sea-level change. The result showed only small changes on a global scale[98] that were not statistically significant. For the full water column, the study relates the global change of the ocean heat content to an energy imbalance of 0.64 ± 0.44 Watts m^{-2}.

Closing the sea-level budget regionally remains challenging, and even more so for inferring deep-ocean warming trends. The subtropical South Pacific, however, is an example where the indirect method is confirmed with sparse in situ observations. There, observations indicate a significant heat uptake in depths below 2,000 m (ref. [99]), attributed to long-term changes in atmospheric circulation driving the deep-reaching circulation[99]. To place tighter constraints on the deep-ocean warming will require spatiotemporally improved observations; such as more accurate gravity fields, improved altimetry estimates near the coast and in polar regions, Argo measurements of deep-ocean and ice regions, and improved estimates of glacial-isostatic adjustment.

Ocean dynamics and overturning circulation. Over the oceans, GRACE measures changes in the mass of the total water column exerted on the ocean floor—the ocean bottom pressure (OBP). From spatial OBP gradients, geostrophic bottom currents can be derived where very few in-situ bottom pressure observations exist. In addition, in-situ sensors cannot provide reliable long-term observations due to chronic sensor drift. GRACE has overcome this severe spatial sampling and temporal resolution problem. The data have been used to infer large-scale oceanic transports on a global, continuous and month-to-month basis[100]. This is particularly useful in remote areas like the Southern Ocean, where in-situ data are extremely sparse and often limited to a few ship transects or repeat-measurements at single locations, such as the Drake Passage.

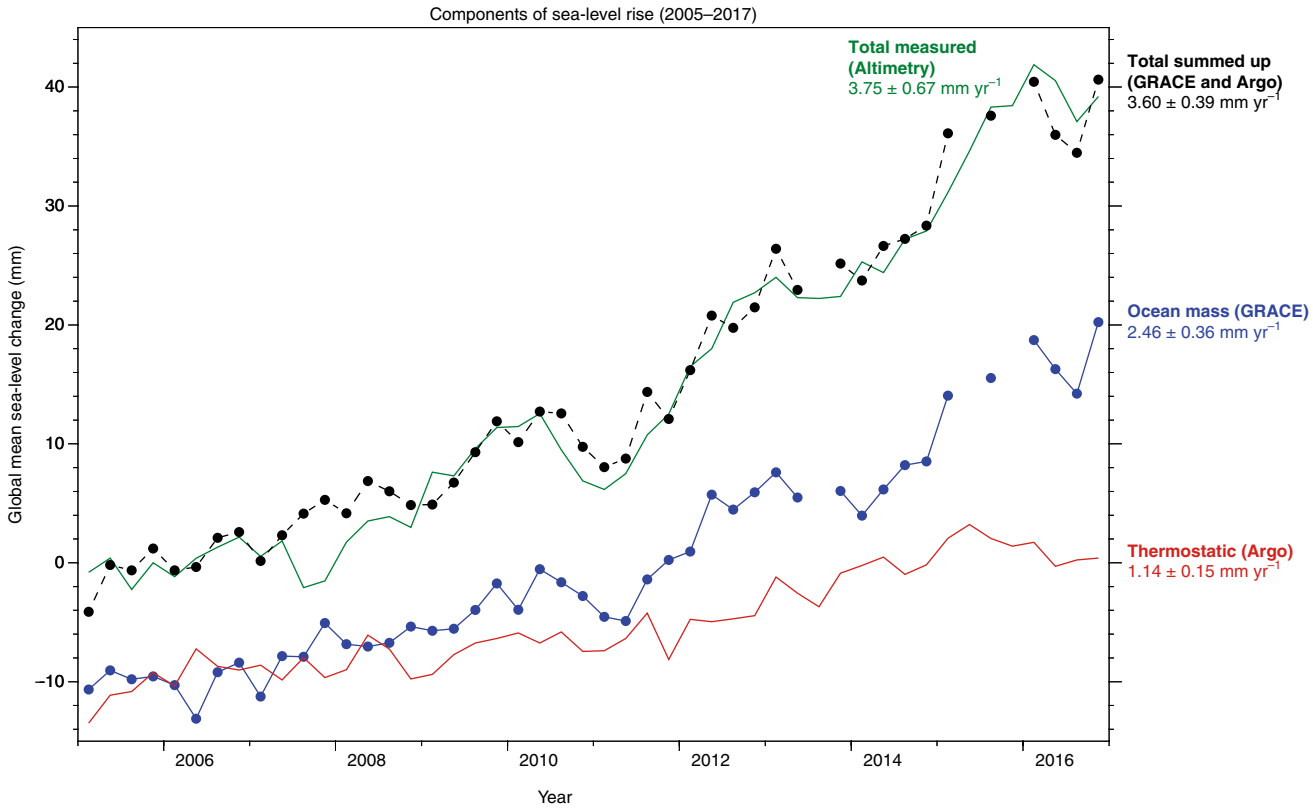

Fig. 4 | Global mean sea-level observed with satellite altimetry, GRACE and Argo floats between 2005 and 2016. Shown are the observed sea-level changes from altimetry (green) and the total sea-level change (black) calculated as the sum of the mass (blue) and volume (red) components. The ocean mass changes are recovered with GRACE and temperature-driven volume (thermosteric) changes are estimated from Argo floats. The black dashed line shows the sum of the mass and volume changes. The values represent three-month (seasonal means), that is: January, February, March; April, May, June; July, August, September; October, November, December. Updated from Chambers et al.[94]. Details on the data shown are presented in 'Data availability'.

As an example, for the Antarctic Circumpolar Current (ACC), bottom currents derived from GRACE were used to estimate the barotropic transport variations of the ACC, which varies significantly on annual to interannual time scales[101,102]. High-resolution models of the ACC, in turn, demonstrate the role of the current in modulating melting of West Antarctic ice shelves through Circumpolar Deep Water (CDW) intruding onto the Antarctic continental shelves[103].

GRACE is particularly important for Arctic Ocean considerations, where perpetual sea-ice cover limits both the sampling of sea-surface heights with altimeters and the use of Argo floats. In addition, altimetry satellites are often placed into inclined orbits, typically lacking coverage higher than latitude 66°. OBP from GRACE, together with ocean modelling, showed that wintertime mass increase in the Arctic Ocean is mainly a consequence of southerly winds through the Fram Strait and, to a lesser extent, through Bering Strait, causing northward geostrophic current anomalies[104]. Moreover, GRACE and ocean modelling showed that non-seasonal mass variations in the Arctic are an effect of the wind-driven redistribution of water, and are not caused by modulations in fresh-water flux[105].

In the northwestern part of the Pacific, GRACE allowed the inference of barotropic variations of large-scale oceanic gyre circulations, which act in periods of days to several years[106,107] in response to changes in the surface wind-stress over the whole North Pacific Region[108]. The results helped to improve the representation of the high-frequency general ocean circulation in global numerical models that are also used as background information in the GRACE gravity field determination[109]. Recent resolution improvements of the GRACE-based bottom pressure estimates even allowed characterization of the spin-up and slow-down of the much smaller Argentine Gyre, which is energized by interactions between the mean flow of the ACC and the local meso-scale eddy field[110].

The Atlantic Meridional Overturning Circulation (AMOC) is a major feature of Earth's climate system, and is essential for Earth's northward ocean-heat transport. It also has a strong bottom-current associated with the deep return flow of North Atlantic Deep Water that provides an accurate measure of the overall AMOC transport. Landerer et al.[111] have recently demonstrated that interannual fluctuations in this lower limb of the AMOC can be derived from GRACE-based OBP variations. This opens the prospect of using satellite gravimeter observations to monitor this important current feature on a broader scale to provide crucial information on its long-term evolution.

Climate service applications

Apart from improving our understanding of climate system components, the GRACE time series of mass storage changes have been used to support an operational climate service. The limitation of the coarse spatial and temporal resolution of the GRACE data for agricultural and societal needs can be overcome by data assimilation into models. Recently, progress has been made in shortening the time lag of GRACE-data availability to near-real-time, breaking ground for new climate forecast services.

Operational drought monitoring. Drought monitoring tools are highly dependent on the availability and quality of precipitation, streamflow, and other observations and indicators of water availability. For example, the premier drought-monitoring tool in the

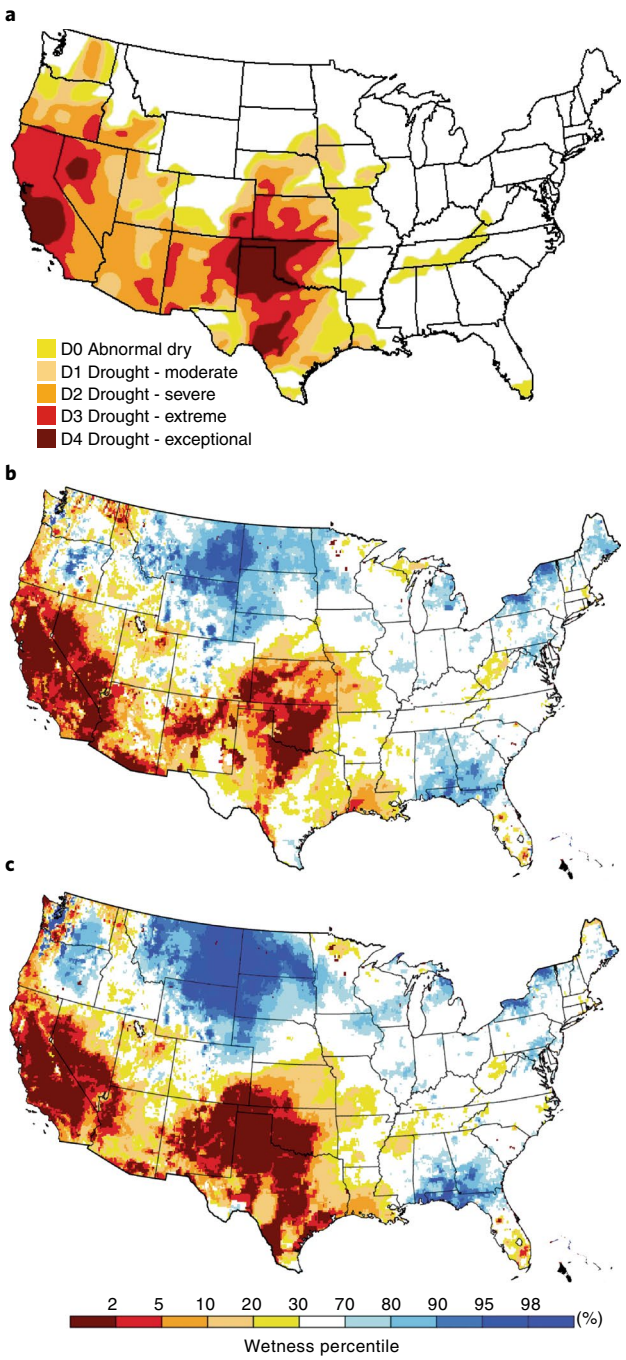

Fig. 5 | Operational drought monitoring supported by GRACE. a–c, Comparison of the USDM map for 20 May 2014 (**a**) with the GRACE data-assimilation-based root-zone soil moisture (**b**) and shallow groundwater wetness/drought indicators for 19 May 2014 (**c**). The scale bar for **b** and **c** describes current wet or dry conditions, expressed as a percentile showing the probability of a given location being dryer at present than at the same time of year during the period of record from 1948 to the present.

United States is the US Drought Monitor (USDM; http://drought.unl.edu/), which provides weekly maps of drought conditions based on a synthesis of in situ data, remote sensing products, and reports from state climatologists and other local experts[112]. Initially the USDM incorporated almost no information on groundwater or terrestrial water storage, and only modelled estimates of soil moisture. In 2011, NASA scientists began to deliver wetness/drought indicators for shallow groundwater and surface- and root-zone soil moisture based on the assimilation of GRACE terrestrial water storage data into a land-surface model[82]. Integration of GRACE TWS data and other observations within a land-data assimilation system has been shown to produce significant improvement in the accuracy of the results. In addition, the assimilation takes advantage of the higher resolutions and increased timeliness of the meteorological fields and models, enabling spatial, temporal and vertical downscaling of GRACE TWS data[75,113]. Gridded maps are now routinely produced at 0.125° within 24 hours of real-time for operational drought monitoring (Fig. 5) (https://nasagrace.unl.edu, last accessed 2 April 2019).

Flood forecasting developments. The use of gravity to detect water-saturated storage conditions in soils has led to an application of GRACE in the monitoring of regional 'flood potential'[45,81,113]. To be most effective, flood forecasting systems require near-real time data to estimate the probability of flood events and to predict their evolution for application in risk and emergency management. The European-Union-funded European Gravity Service for Improved Emergency Management (EGSIEM) project (http://egsiem.eu/, last accessed 2 April 2019) has developed such daily near-real-time gravity products[114], along with GRACE-based wetness indicators. Operational test runs were performed between April and June of 2017, within DLR's Centre for Satellite-based Crisis Information, complemented by hindcast experiments of historical floods, such as the Danube flood events of 2006 and 2010 (ref. [115]). The historical flood analysis demonstrated a significant improvement in early flood-warning using GRACE-derived wetness indicators. Knowledge of the preconditioning of elevated water storage markedly increased the lead times of early flood-warning by up to six weeks prior to peak flow, for example, for the flooding of the Mississippi in 2011 (ref. [81]). The GRACE-derived wetness indicators were also included in a pre-operational way in the Forecast Viewer of the Global Flood Awareness System (GloFAS; http://www.globalfloods.eu/, last accessed 2 April 2019), jointly developed by the European Commission and the European Centre for Medium-Range Weather Forecasts (ECMWF). Recent studies have also demonstrated the effectiveness of assimilated GRACE TWS measurements for seasonal wildfire prediction in the United States[116].

Continuation of the mass transport observations

As the GRACE mission results became accepted, the user community strongly recommended continuation of the mass transport time series[117,118], prioritizing improvements of the satellites and prolonging the measurement over revolutionizing the mission concept with the risk of multi-year gaps in the temporal coverage. NASA and GFZ German Research Centre for Geosciences responded to this user request in 2010, and on 22 May 2018, the successor mission GRACE-FO (Follow-On) was successfully launched from Vandenberg Airforce Base, California, on a Space-X Falcon 9 rocket (https://youtu.be/Tvdz5yFSwCY, last accessed 4 September 2018).

The GRACE-Follow On Mission. While the nominal mission lifetime is again five years, additional operation lifetime is expected based on satellite and instrument design and the influence of solar activity on the atmospheric-induced decay of the spacecraft. During a significant portion of the GRACE mission, the solar flux was very benign, leading to reduced drag decay—a condition that may not repeat itself in the coming years of GRACE-FO.

The GRACE-FO satellites are equipped with evolved versions of GRACE instrumentation (K-band ranging system, GPS, star camera and accelerometer); but the mission also features a novel laser ranging interferometer (LRI)[119], measuring the satellite-to-satellite distance in parallel with the K-band instrument. The LRI has a design precision that is approximately 26-times better than

the K-band ranging system on GRACE[119]—even though the quality of the GRACE and GRACE-FO gravity fields depend on a suite of measurements, as explained in Box 1, the LRI has the potential to increase the accuracy[120]. Successful demonstration of the LRI will establish its potential for use in future GRACE-like gravity missions[121]. However, future mission concepts go beyond developments in instrumentation. Studies show the potential of constellations of satellite pairs for improving the temporal- and spatial-resolution limitations associated with the single pair missions[122,123]. The orbit constellation approach would open new possibilities to directly measure the short-term mass fluctuations that, to some extent, degrade current gravity-field solutions.

Relevance for climate sciences and climate services. Within 15 years, GRACE has evolved from a pioneering concept demonstration into a system for reliably delivering mass transport products. These data and products enabled over two thousand peer-reviewed studies (archives listed in 'Data availability'), of which many are cited in the International Panel on Climate Change Fifth Assessment Report[39], as they significantly contributed to our understanding of climate change. Currently, GRACE mass transport data directly or indirectly contribute to many essential climate variables (ECVs) and should be adopted as a primary ECV of the Global Climate Observing System[124].

Continuing data collection with GRACE-FO will be essential to attribute anthropogenic impacts on ice-loss, sea-level rise and ocean heat uptake, and to quantify global changes in the severity and frequency of droughts and flood events. More accurate gravity fields provided in near-real-time would stimulate new climate service applications that are crucial to regional water-management, flood, drought and snow/ice-melt prediction, providing a database for political decisions or emergency management.

Recognizing the important and versatile utility for satellite gravity observations for Earth science, the recent 2017 NASA Decadal Survey[117] (https://science.nasa.gov/earth-science/decadal-surveys) has recommended a 'mass change continuity mission' among the top five priorities for continued Earth observations. In retrospect, the launch of GRACE on 17 March 2002 provided a truly unique variable to the suite of Earth observations—the mission's legacy of a 15-year record of mass transport in the climate system will serve as an essential baseline for future generations.

Data availability

The GRACE data used in this paper are freely available from the websites of the Science Data Systems Centres. The GRACE gravity field data products (Level 2 data) as well as supporting documentation may be accessed at http://podaac.jpl.nasa.gov/grace and http://isdc.gfz-potsdam.de/grace. User-friendly, gridded maps of mass change (Level 3 data) are available from https://grace.jpl.nasa.gov/ (JPL), http://www2.csr.utexas.edu/grace/ (CSR) and http://gravis.gfz-potsdam.de/home (GFZ). GRACE Follow-On data will be provided through the same portals once available. The reader is encouraged to use all data sets available.

A list of GRACE-related publications is available under https://grace.jpl.nasa.gov/publications/ and https://www.gfz-potsdam.de/en/grace/. Videos of the GRACE-Follow On pre-launch briefing and the launch are available under https://www.youtube.com/watch?v=qYJt-6uHVcM and https://www.youtube.com/watch?v=I_0GgKfwCSk, respectively (both sources last accessed September 15, 2018).

The figures and updates to published values presented in this paper are based on the following data sets and processing.

Figure 1: the plot is based on the 1-arc degree mascon solution by CSR RL05M[5]. A linear trend, annual and semi-annual model is fit to each pixel for the entire mission duration, assuming temporally uniform uncertainties. The temporal linear part of that fit is mapped in a and b the standard deviation shown in c is calculated after the removal of the temporal linear trend. The trends have been corrected for glacial-isostatic adjustment using the ICE5G model of Peltier et al.[13] computed by A et al.[125].

Figure 2 and 'Ice sheets and glaciers': time series of ice-sheet mass change are based on GRACE Level 2 data of CSR RL05 obtained with an inversion approach based on forward modelling[19,126]. For Antarctica the GIA correction is AGE1 (ref. [126]) (48 ± 28 Gt yr^{-1}), for Greenland it is GGG1D (ref. [127])(17 Gt yr^{-1}). Uncertainties are calculated based on the formal monthly uncertainties provided by the processing centres, scaled by the root mean square (RMS) residual after subtracting temporal fluctuations longer than three months. Temporal linear trends for the entire GRACE period are estimated using uncertainty-weighted least squares. Annual balances are estimated using an unweighted piecewise linear model with breakpoints on 1 January. Uncertainties for the temporal linear trends and the annual balances are obtained by error propagation.

Figure 3 and 'Terrestrial water storage': time series of the zonal mean of terrestrial water storage anomalies in mid-latitudes are based on CSR RL05M Mascons[5]. Uncertainties are calculated as RMS residual of the zonal mean after subtracting the linear trend, offset, annual and sub-annual temporal components and fluctuations longer than five months. The RMS uncertainty (2 cm equivalent water height along the latitude, 2σ) is then used to scale the formal, time-dependent uncertainties provided by the processing centre CSR. Then the temporal model is refit and propagated uncertainties are calculated. The annual amplitude is shown on the right part of the figure. The anomalies shown in the left part of the figure are the residuals with respect to the fitted temporal model.

Figure 4 and 'Sea-level change and ocean dynamics': Global Mean Sea-level (GMSL) and its components. GSML from altimetry is based on data provided by the University of Colorado (http://sea-level/colorado.edu)[89]. Ocean mass changes are derived from GRACE Level 2 data of three processing centres (CSR RL05, JPL RL05 and GFZ RL05) using an averaging kernel method and scaling[100], available from the University of South Florida (http://xena.marine.usf.edu/~chambers/SatLab/Home.html). Global mean steric sea level anomalies are based on Argo data provided by the National Oceanic and Atmospheric Administration (NOAA; https://www.nodc.noaa.gov/OC5/3M_HEAT_CONTENT/basin_fsl_data.html). To unify the temporal sampling, we adopt three-month (seasonal) averages, which is limited by the sampling period of the Argo data obtained from NOAA. These were computed after first fitting and removing annual and semi-annual sinusoids from the altimetry and GRACE monthly averages. An annual and semi-annual sinusoid was also estimated and removed from the three-month thermometric time-series for consistency. The correction for glacial-isostatic adjustment to the GRACE data is based on the ICE5G ice model[13,] computed by A et al.[125]. Further details can be found in Chambers et al.[94].

Received: 28 September 2018; Accepted: 12 March 2019;
Published online: 15 April 2019

References

1. Tapley, B. D., Bettadpur, S., Watkins, M. & Reigber, C. The gravity recovery and climate experiment: Mission overview and early results. *Geophys. Res. Lett.* **31**, L09607 (2004).
2. National Research Council. *Satellite gravity and the geosphere: contributions to the study of the solid Earth and its fluid envelopes* (National Acad. Press, 1997).
3. Marti, U. (ed) *Gravity, geoid and height systems: Proceedings of the IAG Symposium GGHS2012, October 9–12, 2012, Venice, Italy* (Springer, 2015).
4. Tapley, B. D. GRACE measurements of mass variability in the Earth system. *Science* **305**, 503–505 (2004).
5. Save, H., Bettadpur, S. & Tapley, B. D. High-resolution CSR GRACE RL05 mascons. *J. Geophys. Res. Solid Earth* **121**, 7547–7569 (2016).
6. Luthcke, S. B. et al. Recent Greenland ice mass loss by drainage system from satellite gravity observations. *Science* **314**, 1286–1289 (2006).

7. Watkins, M. M., Wiese, D. N., Yuan, D.-N., Boening, C. & Landerer, F. W. Improved methods for observing Earth's time variable mass distribution with GRACE using spherical cap mascons. *J. Geophys. Res. Solid Earth* **120**, 2648–2671 (2015).
8. van den Broeke, M. et al. Partitioning recent Greenland mass loss. *Science* **326**, 984–986 (2009).
9. Gardner, A. S. et al. A reconciled estimate of glacier contributions to sea level rise: 2003 to 2009. *Science* **340**, 852–857 (2013).
10. Shepherd, A. et al. Mass balance of the Antarctic Ice Sheet from 1992 to 2017. *Nature* **556**, 219–222 (2018).
11. Vaughan, D. G. et al. in *Climate Change 2013: The Physical Science Basis* (eds. Stocker, T. F. et al.) 317–382 (IPCC, Cambridge Univ. Press, 2013).
12. Rignot, E., Velicogna, I., van den Broeke, M. R., Monaghan, A. & Lenaerts, J. T. Acceleration of the contribution of the Greenland and Antarctic ice sheets to sea level rise. *Geophys. Res. Lett.* **38**, L05503 (2011).
13. Peltier, W. R. Global glacial isostasy and the surface of the ice-age Earth: the ICE-5G (VM2) model and GRACE. *Annu Rev. Earth Planet Sci.* **32**, 111–149 (2004).
14. Caron, L. et al. GIA model statistics for GRACE hydrology, cryosphere, and ocean science. *Geophys. Res. Lett.* **45**, 2203–2212 (2018).
15. Velicogna, I. & Wahr, J. Greenland mass balance from GRACE. *Geophys. Res. Lett.* **32**, L18505 (2005).
16. Velicogna, I. & Wahr, J. Measurements of time-variable gravity show mass loss in Antarctica. *Science* **311**, 1754–1756 (2006).
17. Wouters, B., Chambers, D. & Schrama, E. J. O. GRACE observes small-scale mass loss in Greenland. *Geophys. Res. Lett.* **35**, L20501 (2008).
18. Chen, J. L., Wilson, C. R., Blankenship, D. D. & Tapley, B. D. Antarctic mass rates from GRACE. *Geophys. Res. Lett.* **33**, L11502 (2006).
19. Sasgen, I. et al. Timing and origin of recent regional ice-mass loss in Greenland. *Earth Planet. Sci. Lett.* **333**, 293–303 (2012).
20. Velicogna, I., Sutterley, T. C. & Van Den Broeke, M. R. Regional acceleration in ice mass loss from Greenland and Antarctica using GRACE time-variable gravity data. *Geophys. Res. Lett.* **41**, 8130–8137 (2014).
21. Wouters, B. et al. Limits in detecting acceleration of ice sheet mass loss due to climate variability. *Nat. Geosci.* **6**, 613–616 (2013).
22. WCRP Global Sea Level Budget Group. Global sea-level budget 1993–present, *Earth Syst. Sci. Data* **10**, 1551–1590 (2018).
23. Hanna, E. et al. Atmospheric and oceanic climate forcing of the exceptional Greenland ice sheet surface melt in summer 2012. *Int. J. Climatol.* **34**, 1022–1037 (2014).
24. Sasgen, I., Dobslaw, H., Martinec, Z. & Thomas, M. Satellite gravimetry observation of Antarctic snow accumulation related to ENSO. *Earth Planet. Sci. Lett.* **299**, 352–358 (2010).
25. Boening, C., Lebsock, M., Landerer, F. & Stephens, G. Snowfall-driven mass change on the East Antarctic ice sheet. *Geophys. Res. Lett.* **39**, L21501 (2012).
26. Mémin, A., Flament, T., Alizier, B., Watson, C. & Rémy, F. Interannual variation of the Antarctic Ice Sheet from a combined analysis of satellite gravimetry and altimetry data. *Earth Planet. Sci. Lett.* **422**, 150–156 (2015).
27. Behrangi, A., Gardner, A. S., Reager, J. T. & Fisher, J. B. Using GRACE to constrain precipitation amount over cold mountainous basins. *Geophys. Res. Lett.* **44**, 219–227 (2017).
28. Arendt, A. et al. Analysis of a GRACE global mascon solution for Gulf of Alaska glaciers. *J. Glaciol.* **59**, 913–924 (2013).
29. Gardner, A. S. et al. Sharply increased mass loss from glaciers and ice caps in the Canadian Arctic Archipelago. *Nature* **473**, 357–360 (2011).
30. Lenaerts, J. T. et al. Irreversible mass loss of Canadian Arctic Archipelago glaciers. *Geophys. Res. Lett.* **40**, 870–874 (2013).
31. Tamisiea, M. E., Leuliette, E. W., Davis, J. L. & Mitrovica, J. X. Constraining hydrological and cryospheric mass flux in southeastern Alaska using space-based gravity measurements. *Geophys. Res. Lett.* **32**, L20501 (2005).
32. Luthcke, S. B., Arendt, A. A., Rowlands, D. D., McCarthy, J. J. & Larsen, C. F. Recent glacier mass changes in the Gulf of Alaska region from GRACE mascon solutions. *J. Glaciol.* **54**, 767–777 (2008).
33. Chen, J. L., Wilson, C. R., Tapley, B. D., Blankenship, D. D. & Ivins, E. R. Patagonia icefield melting observed by Gravity Recovery and Climate Experiment (GRACE). *Geophys. Res. Lett.* **34**, L22501 (2007).
34. Ivins, E. R. et al. On-land ice loss and glacial isostatic adjustment at the Drake Passage: 2003–2009. *J. Geophys. Res. Solid Earth* **116**, B02403 (2011).
35. Jacob, T., Wahr, J., Pfeffer, W. T. & Swenson, S. Recent contributions of glaciers and ice caps to sea level rise. *Nature* **482**, 514–518 (2012).
36. Reager, J. T. et al. A decade of sea level rise slowed by climate-driven hydrology. *Science* **351**, 699–703 (2016).
37. Rodell, M. et al. Emerging trends in global freshwater availability. *Nature* **557**, 651–659 (2018).
38. Held, I. M. & Soden, B. J. Robust Responses of the Hydrological Cycle to Global Warming. *J. Clim.* **19**, 5686–5699 (2006).
39. IPCC *Climate Change 2013: The Physical Science Basis* (eds Stocker, T. F. et al.) (Cambridge Univ. Press, 2013).
40. Richey, A. S. et al. Uncertainty in global groundwater storage estimates in a total groundwater stress framework. *Water Resour. Res.* **51**, 5198–5216 (2015).
41. Jensen, L., Rietbroek, R. & Kusche, J. Land water contribution to sea level from GRACE and Jason-1 measurements. *J. Geophys. Res. Oceans* **118**, 212–226 (2013).
42. Humphrey, V., Gudmundsson, L. & Seneviratne, S. I. Assessing global water storage variability from GRACE: Trends, seasonal cycle, subseasonal anomalies and extremes. *Surv. Geophys.* **37**, 357–395 (2016).
43. Rietbroek, R., Brunnabend, S.-E., Kusche, J., Schröter, J. & Dahle, C. Revisiting the contemporary sea-level budget on global and regional scales. *Proc. Natl Acad. Sci. USA* **113**, 1504–1509 (2016).
44. Scanlon, B. R. et al. Global models underestimate large decadal declining and rising water storage trends relative to GRACE satellite data. *Proc. Natl Acad. Sci. USA* **115**, 1080–1089 (2018).
45. Reager, J. T. & Famiglietti, J. S. Global terrestrial water storage capacity and flood potential using GRACE. *Geophys. Res. Lett.* **36**, L23402 (2009).
46. Boening, C., Willis, J. K., Landerer, F. W., Nerem, R. S. & Fasullo, J. The 2011 La Niña: So strong, the oceans fell. *Geophys. Res. Lett.* **39**, L109602 (2012).
47. Chen, J. L., Wilson, C. R., Tapley, B. D., Yang, Z. L. & Niu, G. Y. 2005 drought event in the Amazon River basin as measured by GRACE and estimated by climate models. *J. Geophys. Res. Solid Earth* **114**, B05404 (2009).
48. Long, D. et al. GRACE satellite monitoring of large depletion in water storage in response to the 2011 drought in Texas. *Geophys. Res. Lett.* **40**, 3395–3401 (2013).
49. Thomas, A. C., Reager, J. T., Famiglietti, J. S. & Rodell, M. A GRACE-based water storage deficit approach for hydrological drought characterization. *Geophys. Res. Lett.* **41**, 1537–1545 (2014).
50. Rodell, M. et al. The observed state of the water cycle in the early twenty-first century. *J. Clim.* **28**, 8289–8318 (2015).
51. Rodell, M., Famiglietti, J.S., Chambers, D.P. & Wahr, J. in *State of the Climate in 2010* (eds Blunden, J., Arndt, D. S. & Baringer, M.O.) S50–S51 (Bull. Amer. Meteor. Soc., 2011).
52. Eicker, A., Forootan, E., Springer, A., Longuevergne, L. & Kusche, J. Does GRACE see the terrestrial water cycle "intensifying"? *J. Geophys. Res. Atmospheres* **121**, 733–745 (2016).
53. Humphrey, V. et al. Sensitivity of atmospheric CO2 growth rate to observed changes in terrestrial water storage. *Nature* **560**, 628–631 (2018).
54. Rodell, M., McWilliams, E. B., Famiglietti, J. S., Beaudoing, H. K. & Nigro, J. Estimating evapotranspiration using an observation based terrestrial water budget. *Hydrol. Process.* **25**, 4082–4092 (2011).
55. Sheffield, J., Ferguson, C. R., Troy, T. J., Wood, E. F. & McCabe, M. F. Closing the terrestrial water budget from satellite remote sensing. *Geophys. Res. Lett.* **36**, L07403 (2009).
56. Yeh, P. J.-F., Swenson, S. C., Famiglietti, J. S. & Rodell, M. Remote sensing of groundwater storage changes in Illinois using the Gravity Recovery and Climate Experiment (GRACE). *Water Resour. Res.* **42**, W12203 (2006).
57. Rodell, M. et al. Estimating groundwater storage changes in the Mississippi River basin (USA) using GRACE. *Hydrogeol. J.* **15**, 159–166 (2007).
58. Rodell, M., Velicogna, I. & Famiglietti, J. S. Satellite-based estimates of groundwater depletion in India. *Nature* **460**, 999–1002 (2009).
59. Longuevergne, L., Scanlon, B. R. & Wilson, C. R. GRACE Hydrological estimates for small basins: Evaluating processing approaches on the High Plains Aquifer, USA. *Water Resour. Res.* **46**, W11517 (2010).
60. Famiglietti, J. S. et al. Satellites measure recent rates of groundwater depletion in California's Central Valley. *Geophys. Res. Lett.* **38**, L03403 (2011).
61. Voss, K. A. et al. Groundwater depletion in the Middle East from GRACE with implications for transboundary water management in the Tigris-Euphrates-Western Iran region. *Water Resour. Res.* **49**, 904–914 (2013).
62. Castle, S. L. et al. Groundwater depletion during drought threatens future water security of the Colorado River Basin. *Geophys. Res. Lett.* **41**, 5904–5911 (2014).
63. Sultan, M., Ahmed, M., Wahr, J., Yan, E. & Emil, M. K. Monitoring aquifer depletion from space: case studies from the saharan and arabian aquifers. *Remote Sens. Terr. Water Cycle* **206**, 349 (2014).
64. Doell, P., Mueller Schmied, H., Schuh, C., Portmann, F. T. & Eicker, A. Global-scale assessment of groundwater depletion and related groundwater abstractions: combining hydrological modeling with information from well observations and GRACE satellites. *Water Resour. Res.* **50**, 5698–5720 (2014).
65. Famiglietti, J. S. The global groundwater crisis. *Nat. Clim. Change* **4**, 945–948 (2014).
66. Ramillien, G. et al. Time variations of the regional evapotranspiration rate from Gravity Recovery and Climate Experiment (GRACE) satellite gravimetry. *Water Resour. Res.* **42**, W10403 (2006).
67. Syed, T. H. et al. Total basin discharge for the Amazon and Mississippi River basins from GRACE and a land-atmosphere water balance. *Geophys. Res. Lett.* **32**, L24404 (2005).

68. Swenson, S. & Wahr, J. Estimating large-scale precipitation minus evapotranspiration from GRACE satellite gravity measurements. *J. Hydrometeorol.* **7**, 252–270 (2006).
69. Syed, T. H., Famiglietti, J. S. & Chambers, D. P. GRACE-based estimates of terrestrial freshwater discharge from basin to continental scales. *J. Hydrometeorol.* **10**, 22–40 (2009).
70. Niu, G.-Y. & Yang, Z.-L. Assessing a land surface model's improvements with GRACE estimates. *Geophys. Res. Lett.* **33**, L07401 (2006).
71. Lo, M.-H., Famiglietti, J. S., Yeh, P.-F. & Syed, T. H. Improving parameter estimation and water table depth simulation in a land surface model using GRACE water storage and estimated base flow data. *Water Resour. Res.* **46**, W05517 (2010).
72. Swenson, S. C. & Lawrence, D. M. A GRACE-based assessment of interannual groundwater dynamics in the Community Land Model. *Water Resour. Res.* **51**, 8817–8833 (2015).
73. Güntner, A. et al. A global analysis of temporal and spatial variations in continental water storage. *Water Resour. Res.* **43**, W05416 (2007).
74. Sun, A. Y., Green, R., Swenson, S. & Rodell, M. Toward calibration of regional groundwater models using GRACE data. *J. Hydrol.* **422**, 1–9 (2012).
75. Zaitchik, B. F., Rodell, M. & Reichle, R. H. Assimilation of GRACE terrestrial water storage data into a land surface model: Results for the Mississippi River basin. *J. Hydrometeorol.* **9**, 535–548 (2008).
76. Forman, B. A., Reichle, R. H. & Rodell, M. Assimilation of terrestrial water storage from GRACE in a snow-dominated basin. *Water Resour. Res.* **48**, W01507 (2012).
77. van Dijk, A. I., Renzullo, L. J., Wada, Y. & Tregoning, P. A global water cycle reanalysis (2003–2012) merging satellite gravimetry and altimetry observations with a hydrological multi-model ensemble. *Hydrol. Earth Syst. Sci.* **18**, 2955–2973 (2014).
78. Eicker, A., Schumacher, M., Kusche, J., Döll, P. & Schmied, H. M. Calibration/data assimilation approach for integrating GRACE data into the WaterGAP Global Hydrology Model (WGHM) using an ensemble Kalman filter: First results. *Surv. Geophys.* **35**, 1285–1309 (2014).
79. Girotto, M., De Lannoy, G. J., Reichle, R. H. & Rodell, M. Assimilation of gridded terrestrial water storage observations from GRACE into a land surface model. *Water Resour. Res.* **52**, 4164–4183 (2016).
80. Trautmann, T. et al. Understanding terrestrial water storage variations in northern latitudes across scales. *Hydrol. Earth Syst. Sci.* **22**, 4061–4082 (2018).
81. Reager, J. T., Thomas, B. F. & Famiglietti, J. S. River basin flood potential inferred using GRACE gravity observations at several months lead time. *Nat. Geosci.* **7**, 588–592 (2014).
82. Houborg, R., Rodell, M., Li, B., Reichle, R. & Zaitchik, B. F. Drought indicators based on model-assimilated Gravity Recovery and Climate Experiment (GRACE) terrestrial water storage observations. *Water Resour. Res.* **48**, W07525 (2012).
83. Phillips, T., Nerem, R. S., Fox-Kemper, B., Famiglietti, J. S. & Rajagopalan, B. The influence of ENSO on global terrestrial water storage using GRACE. *Geophys. Res. Lett.* **39**, L16705 (2012).
84. Ni, S. et al. Global Terrestrial Water Storage Changes and Connections to ENSO Events. *Surv. Geophys.* **39**, 1–22 (2018).
85. Kusche, J., Eicker, A., Forootan, E., Springer, A. & Longuevergne, L. Mapping probabilities of extreme continental water storage changes from space gravimetry. *Geophys. Res. Lett.* **43**, 8026–8034 (2016).
86. Zhang, L., Dobslaw, H., Dahle, C., Sasgen, I. & Thomas, M. Validation of MPI-ESM decadal hindcast experiments with terrestrial water storage variations as observed by the GRACE satellite mission. *Meteor. Z.* **25**, 685–694 (2015).
87. Jevrejeva, S., Jackson, L. P., Riva, R. E., Grinsted, A. & Moore, J. C. Coastal sea level rise with warming above 2°C. *Proc. Natl Acad. Sci. USA* **113**, 13342–13347 (2016).
88. Alley, R. B., Clark, P. U., Huybrechts, P. & Joughin, I. Ice-sheet and sea-level changes. *Science* **310**, 456–460 (2005).
89. Nerem, R. S. et al. Climate-change-driven accelerated sea-level rise detected in the altimeter era. *Proc. Natl Acad. Sci. USA* **115**, 201717312 (2018).
90. Riser, S. C. et al. Fifteen years of ocean observations with the global Argo array. *Nat. Clim. Change* **6**, 145–153 (2016).
91. von Schuckmann, K. et al. An imperative to monitor Earth's energy imbalance. *Nat. Clim. Change* **6**, 138–144 (2016).
92. Willis, J. K., Roemmich, D. & Cornuelle, B. Interannual variability in upper ocean heat content, temperature, and thermosteric expansion on global scales. *J. Geophys. Res. Oceans* **109**, C12036 (2004).
93. Chambers, D. P., Wahr, J. & Nerem, R. S. Preliminary observations of global ocean mass variations with GRACE. *Geophys. Res. Lett.* **31**, (2004).
94. Chambers, D. P. et al. in *Integrative Study of the Mean Sea Level and Its Components* (eds Cazenave, A. et al.) 315–333 (Springer, 2017).
95. Ngo-Duc, T., Laval, K., Polcher, J. & Cazenave, A. Contribution of continental water to sea level variations during the 1997–1998 El Niño–Southern Oscillation event: comparison between Atmospheric Model Intercomparison Project simulations and TOPEX/Poseidon satellite data. *J. Geophys. Res. Atmospheres* **110**, D09103 (2005).
96. Fasullo, J. T., Boening, C., Landerer, F. W. & Nerem, R. S. Australia's unique influence on global sea level in 2010–2011. *Geophys. Res. Lett.* **40**, 4368–4373 (2013).
97. Roemmich, D. et al. Unabated planetary warming and its ocean structure since 2006. *Nat. Clim. Change* **5**, 240–245 (2015).
98. Llovel, W., Willis, J. K., Landerer, F. W. & Fukumori, I. Deep-ocean contribution to sea level and energy budget not detectable over the past decade. *Nat. Clim. Change* **4**, 1031 (2014).
99. Volkov, D. L., Lee, S.-K., Landerer, F. W. & Lumpkin, R. Decade-long deep-ocean warming detected in the subtropical South Pacific. *Geophys. Res. Lett.* **44**, 927–936 (2017).
100. Johnson, G. C. & Chambers, D. P. Ocean bottom pressure seasonal cycles and decadal trends from GRACE Release-05: Ocean circulation implications. *J. Geophys. Res. Oceans* **118**, 4228–4240 (2013).
101. Zlotnicki, V., Wahr, J., Fukumori, I. & Song, Y. T. Antarctic Circumpolar Current transport variability during 2003–05 from GRACE. *J. Phys. Oceanogr.* **37**, 230–244 (2007).
102. Bergmann, I. & Dobslaw, H. Short-term transport variability of the Antarctic Circumpolar Current from satellite gravity observations. *J. Geophys. Res. Oceans* **117**, C05044 (2012).
103. Nakayama, Y., Menemenlis, D., Zhang, H., Schodlok, M. & Rignot, E. Origin of Circumpolar deep water intruding onto the Amundsen and Bellingshausen Sea continental shelves. *Nat. Commun.* **9**, 3403 (2018).
104. Peralta-Ferriz, C., Morison, J. H., Wallace, J. M., Bonin, J. A. & Zhang, J. Arctic Ocean circulation patterns revealed by GRACE. *J. Clim.* **27**, 1445–1468 (2014).
105. Volkov, D. L. & Landerer, F. W. Nonseasonal fluctuations of the Arctic Ocean mass observed by the GRACE satellites. *J. Geophys. Res. Oceans* **118**, 6451–6460 (2013).
106. Bingham, R. J. & Hughes, C. W. Observing seasonal bottom pressure variability in the North Pacific with GRACE. *Geophys. Res. Lett.* **33**, L08607 (2006).
107. Song, Y. T. & Zlotnicki, V. Subpolar ocean bottom pressure oscillation and its links to the tropical ENSO. *Int. J. Remote Sens.* **29**, 6091–6107 (2008).
108. Petrick, C. et al. Low-frequency ocean bottom pressure variations in the North Pacific in response to time-variable surface winds. *J. Geophys. Res. Oceans* **119**, 5190–5202 (2014).
109. Dobslaw, H. et al. A new high-resolution model of non-tidal atmosphere and ocean mass variability for de-aliasing of satellite gravity observations: AOD1B RL06. *Geophys. J. Int.* **211**, 263–269 (2017).
110. Yao, Y., Chao, B. F., García-García, D. & Luo, Z. Variations of the Argentine Gyre observed in the GRACE time-variable gravity and ocean altimetry measurements. *J. Geophys. Res. Oceans* **123**, 5375–5387 (2018).
111. Landerer, F. W., Wiese, D. N., Bentel, K., Boening, C. & Watkins, M. M. North Atlantic meridional overturning circulation variations from GRACE ocean bottom pressure anomalies. *Geophys. Res. Lett.* **42**, 8114–8121 (2015).
112. Svoboda, M. et al. The drought monitor. *Bull. Am. Meteorol. Soc.* **83**, 1181–1190 (2002).
113. Reager, J. T. et al. Assimilation of GRACE terrestrial water storage observations into a land surface model for the assessment of regional flood potential. *Remote Sens.* **7**, 14663–14679 (2015).
114. Gruber, C. & Gouweleeuw, B. Short-latency monitoring of continental, ocean- and atmospheric mass variations using GRACE intersatellite acceleration. *Geophys. J. Int.* **217**, 714–728 (2019).
115. Gouweleeuw, B. T. et al. Daily GRACE gravity field solutions track major flood events in the Ganges–Brahmaputra Delta. *Hydrol. Earth Syst. Sci.* **22**, 2867 (2018).
116. Jensen, D. et al. The sensitivity of US wildfire occurrence to pre-season soil moisture conditions across ecosystems. *Environ. Res. Lett.* **13**, 014021 (2018).
117. National Academies of Sciences, Engineering, and Medicine. *Thriving on Our Changing Planet: A Decadal Strategy for Earth Observation from Space* (National Acad. Press, 2018).
118. National Research Council. *Earth Science and Applications from Space: National Imperatives for the Next Decade and Beyond* (National Acad. Press, 2007).
119. Sheard, B. S. et al. Intersatellite laser ranging instrument for the GRACE follow-on mission. *J. Geod.* **86**, 1083–1095 (2012).
120. Flechtner, F. et al. in *Remote Sensing and Water Resources* (eds Cazenave, A. et al.) 263–280 (Springer, 2016).
121. Pail, R. et al. Science and user needs for observing global mass transport to understand global change and to benefit society. *Surv. Geophys.* **36**, 743–772 (2015).
122. Wiese, D. N., Nerem, R. S. & Lemoine, F. G. Design considerations for a dedicated gravity recovery satellite mission consisting of two pairs of satellites. *J. Geod.* **86**, 81–98 (2012).

123. Elsaka, B. et al. Comparing seven candidate mission configurations for temporal gravity field retrieval through full-scale numerical simulation. *J. Geod.* **88**, 31–43 (2014).
124. Bojinski, S. et al. The concept of essential climate variables in support of climate research, applications, and policy. *Bull. Am. Meteorol. Soc.* **95**, 1431–1443 (2014).
125. A, G., Wahr, J. & Zhong, S. Computations of the viscoelastic response of a 3-D compressible Earth to surface loading: an application to Glacial Isostatic Adjustment in Antarctica and Canada. *Geophys. J. Int.* **192**, 557–572 (2013).
126. Sasgen, I. et al. Antarctic ice-mass balance 2003 to 2012: regional reanalysis of GRACE satellite gravimetry measurements with improved estimate of glacial-isostatic adjustment based on GPS uplift rates. *Cryosphere* **7**, 1499–1512 (2013).
127. Khan, S. A. et al. Geodetic measurements reveal similarities between post–Last Glacial Maximum and present-day mass loss from the Greenland ice sheet. *Sci. Adv.* **2**, e1600931 (2016).
128. Vishwakarma, B., Devaraju, B. & Sneeuw, N. What is the spatial resolution of GRACE satellite products for hydrology? *Remote Sens.* **10**, 852 (2018).
129. *GRACE-FO Launch Press Kit* (NASA, 2018).

Acknowledgements

The authors acknowledge the influence of J. M. Wahr (formerly of the University of Colorado Boulder, USA) making fundamental contributions, both in theoretical concept and in measurement applications, to the success of the GRACE mission.

C.D., H.D. und F.F. acknowledge funding of the development of the GRACE-Follow On Science Data System by the German Federal Ministry of Education and Research (BMBF) under grant 03F0654A. I.S. acknowledges funding by the Helmholtz Climate Initiative REKLIM (Regional Climate Change), a joint research project of the Helmholtz Association of German Research Centres (HGF) and the German Research Foundation (DFG) through grant SA 1734/4-1. A.G. received funding from the NASA Cryosphere Science program. M.E.T. was supported by CSR discretionary funds.

Author contributions

All authors contributed the writing and editing of the paper; introductory text (B.D.T., C. R., S.B., M.W. and I.S.), 'Ice sheets and glaciers' (I.S., A.G. and I.V.), 'Terrestrial Water Storage' (J.F., M.R., J.T.R, and S.S.), 'Sea-level change and ocean dynamics' (D.C., F.L., C.B., H.D. and I.S.), 'Climate service applications' (F.F., C.D., D.W. and M. R.) and 'Future of mass transport observations' (B.D.T., F.L., M.W., F.F. and I.S.); overall editing and internal review E.R.I. and M.E.T; Box 1 (NASA/JPL, I. S.); Fig. 1 (H.S.), Fig. 2 (I.S.), Fig. 3 (I.S. and M.R.), Fig. 4 (D.C. and I.S.) and Fig. 5 (M.R.). I.S. handled implementing the comments of peer reviewers.

Competing interests

The authors declare no competing interests.

Additional information

Reprints and permissions information is available at www.nature.com/reprints.

Correspondence should be addressed to I.S.

Journal peer review information: *Nature Climate Change* thanks Bryant Loomis and other anonymous reviewer(s) for their contribution to the peer review of this work.